

Pressure-induced structural phase transition and electronic structure of $\text{In}_{1-x}\text{Ga}_x\text{P}$ alloys: a DFT study

Kabita KHOIROM¹, Indrajit SHARMA^{2,*}, Brojen SINGH³, Ramkumar THAPA⁴

¹Department of Physics, Jiri College, Imphal East, Manipur, India

²Department of Physics, Assam University Silchar, Silchar, India

³School of Computational and Integrative Sciences, Jawaharlal Nehru University, New Delhi, India

⁴Department of Physics, Mizoram University, Tanhril, Aizawl, India

Received: 15.06.2018

Accepted/Published Online: 11.03.2019

Final Version: 08.04.2019

Abstract: We present the density functional calculation to study the pressure-induced structural phase transition and electronic structure of $\text{In}_{1-x}\text{Ga}_x\text{P}$ ($x = 0.0, 0.25, 0.5, 0.75, 1$) alloys. We report the optimized structural parameters such as lattice constant, bulk modulus, and derivative of the bulk modulus of the alloys. Our calculation confirms that the alloys in the zinc-blende structure are more stable than in the rock-salt structure. The phase transition study from zinc-blende to rock-salt under pressure shows that the transition pressure increases with an increase in doping concentration. The energy band diagram of the alloys in the zinc-blende phase reveals a direct band gap. However, the alloy at $x = 1$ (GaP) is an indirect band gap compound in agreement with the reported experimental and theoretical results. The alloys that are in the rock-salt structure exhibit a metallic nature.

Key words: Phase transition, electronic structure, density functional theory

1. Introduction

In recent years, the study of III–V binary compound semiconductors has considerably increased in the broad scientific and industrial community due to their potential technological importance. These materials are widely used in the fabrication of optoelectronic and photovoltaic devices [1–3]. Advancement in high-pressure research leads to many theoretical and experimental studies for a better understanding of the structural phase transition and electronic properties of the III–V compounds [4–8]. With an increase in technology, attempts have been made to uncover credible alternatives for improving optoelectronic device performances. Also, the possibility of controlling the physical properties of these alloys in different compositions offers an immense scope of theoretical and experimental studies. Among the III–V semiconductors, InP and GaP have attracted particular attention, and many studies have been performed on these compounds to understand the effects of external influences such as pressure. At ambient pressure, InP and GaP are found to crystallize in a fourfold coordinated zinc-blende structure, and at higher pressure, they undergo a structural phase transition to a sixfold coordinated rock-salt structure [9–13]. To date, there have been various computational methods applied to study these compound semiconductors, but there are not many works in the literature on a detailed theoretical study that explored the structural properties, phase transitions, and electronic structures of $\text{In}_x\text{Ga}_{1-x}\text{P}$ alloys. In the present work, we investigate the pressure-induced structural phase transition and electronic structure of $\text{In}_{1-x}\text{Ga}_x\text{P}$ alloys ($x = 0.0, 0.25, 0.5, 0.75, 1$) and the effect of doping in InP compound with Ga atoms.

*Correspondence: indraofficial@rediffmail.com

2. Computational method

All calculations in the present work are performed using the full potential linearized augmented plane wave (FP-LAPW) method [14] within the framework of density functional theory (DFT) [15–17]. Perdew–Burke–Ernzerhof generalized gradient approximation (PBE-GGA) is used for the exchange-correlation potential [18] as implemented in the WIEN2K code [19]. In the FP-LAPW method, the lattice divides into nonoverlapping spheres called a muffin tin (MT) surrounding each nuclear site and an interstitial region. Inside the muffin tin region, the potential contains both spherical harmonics and radial function. The potential in the interstitial regions (which are outside the muffin tin sphere) expands in plane waves. Convergence occurs at $RMTK_{max} = 9.0$, where RMT is the atomic sphere radii, and K_{max} gives the plane wave cut-off. In the present calculations, Brillouin-zone (BZ) sampling uses $8 \times 8 \times 8$ k mesh points for all the $In_{1-x}Ga_xP$ alloys for x varying from 0.0 to 1 by steps of 0.25.

3. Results and discussion

3.1. Structural properties and phase transition

The DFT-based ab initio method is used for investigating structural properties and phase transitions of $In_{1-x}Ga_xP$ alloys with doping concentration $x = 0.0, 0.25, 0.5, 0.75, 1$. The minimization of total energy concerning the cell parameter is considered as geometrical optimization. The equilibrium lattice parameters and bulk modulus are obtained from the energy versus per unit cell volume curves by fitting to the Birch–Murnaghan equation of states [20]. Figures 1a–1e show the energy versus per unit cell volume curve for the different compositions of the $In_{1-x}Ga_xP$ alloys for both zinc-blende (ZB) and rock-salt (RS) phases. The positions of the different atoms (In/Ga and P) are (0,0,0); (0.25,0.25,0.25) for the ZB phase and (0,0,0); (0.5,0.5,0.5) for the RS structure.

Table 1 summarizes the lattice parameters for the optimized structures of the $In_{1-x}Ga_xP$ alloys ($x = 0.0, 0.25, 0.5, 0.75, 1$). In the literature, the structural data for the starting (at $x = 0.0$) compound InP and the end (at $x = 1$) compound GaP are available for comparison. The calculated optimized structural parameters are in good agreement with other available theoretical and experimental data [21–32], as given in Table 1.

According to Vegard’s law [33], there is a linear relationship between the crystal lattice constant of an alloy and composition x at a constant temperature, which is given by

$$a_{(In_{1-x}Ga_xP)} = x(a_{GaP}) + (1 - x)(a_{InP}), \quad (1)$$

where $a_{(A_{1-x}B_xC)}$ is the lattice constant of the $A_{1-x}B_xC$ alloy, and a_{BC} and a_{AC} are the equilibrium lattice constants of the binary compounds BC and AC, respectively.

In the literature, the experimental and theoretical studies confirm that there is a deviation from Vegard’s law [34–40]. This deviation is addressed in the description of the lattice constant as follows:

$$a_{(In_{1-x}Ga_xP)} = xa_{GaP} + (1 - x)a_{InP} - x(1 - x)b, \quad (2)$$

where the quadratic term b is called the bowing parameter.

The composition dependence of lattice parameter a_o and bulk modulus B_o as compared with Vegard’s prediction is shown in Figures 2a and 2b and Figures 3a and 3b, respectively. Our calculated lattice parameter for the zinc-blende phase shows an almost linear variation with a marginal upward bowing parameter of 0.02823

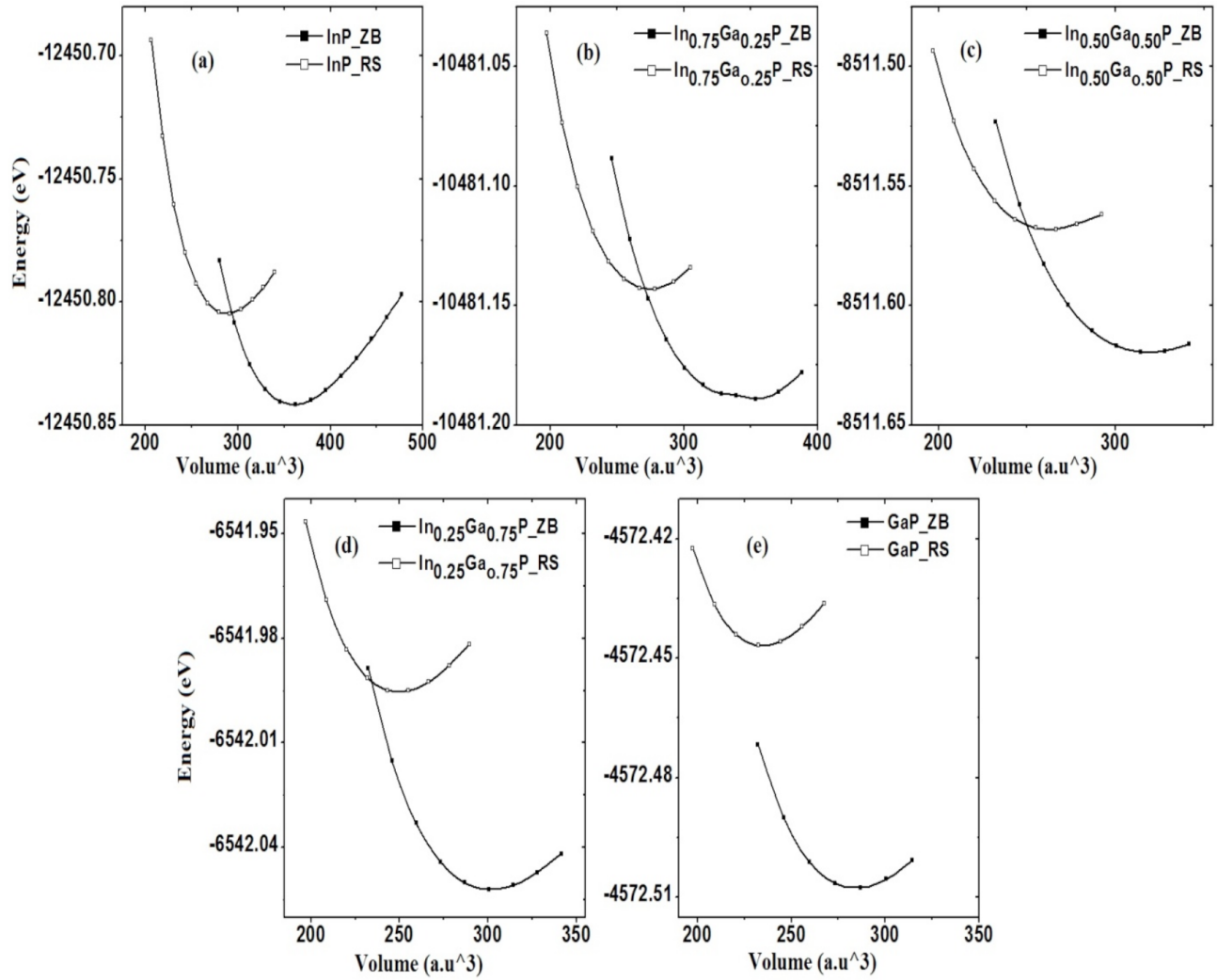


Figure 1. (a, b, c, d, e) Energy versus per unit cell volume of $\text{In}_{1-x}\text{Ga}_x\text{P}$ alloys ($x = 0.0, 0.25, 0.5, 0.75, 1$) in ZB and RS structures.

Table 1. Optimized lattice parameters of $\text{In}_{1-x}\text{Ga}_x\text{P}$ alloys ($x = 0.0, 0.25, 0.50, 0.75, 1$).

		ZB structure			RS structure		
		a_o	B_o	B'	a_o	B_o	B'
InP	Pres. work	5.9	60.5	4.64	5.54	74.78	4.76
	Expt. results	5.90 ²¹ , 5.87 ²²	65.5 ²⁴ , 72.0 ²⁵	4.59 ²³	5.71 ²² , 5.24 ²²	-	-
	Theo. results	5.95 ²³ , 5.94 ²² ,	71.0 ²⁶ , 68.0 ²² ,	4.67 ²⁷ , 4.9 ²² ,	-	-	-
$\text{In}_{0.75}\text{Ga}_{0.25}\text{P}$	Pres. work	5.85	65.16	4.42	5.46	76.75	4.60
$\text{In}_{0.5}\text{Ga}_{0.5}\text{P}$	Pres. work	5.73	67.72	4.46	5.37	78.49	4.70
$\text{In}_{0.25}\text{Ga}_{0.75}\text{P}$	Pres. work	5.63	72.01	4.56	5.28	82.65	4.74
GaP	Pres. work	5.52	77.70	4.34	5.18	88.30	4.84
	Expt. results	5.47 ²⁸ , 5.50 ²⁹ , 5.45 ³⁰	77.2 ²⁹	4.88 ²⁹ ,	-	-	-
	Theo. results	5.54 ³¹ , 5.51 ³² , 5.41 ¹³	90.0 ¹³ , 76.0 ³² ,	4.50 ¹³ , 4.59 ³²	5.16 ² , 5.16 ²⁶	87.3 ² , 87.59 ²⁶	3.78 ² , 4.54 ²⁶

Å and a downward bowing parameter of 0.07189 Å for the rock-salt structure. In the case of bulk modulus, there is a deviation from linearity with an upward bowing parameter of 4.33704 GPa and 11.1624 GPa for both

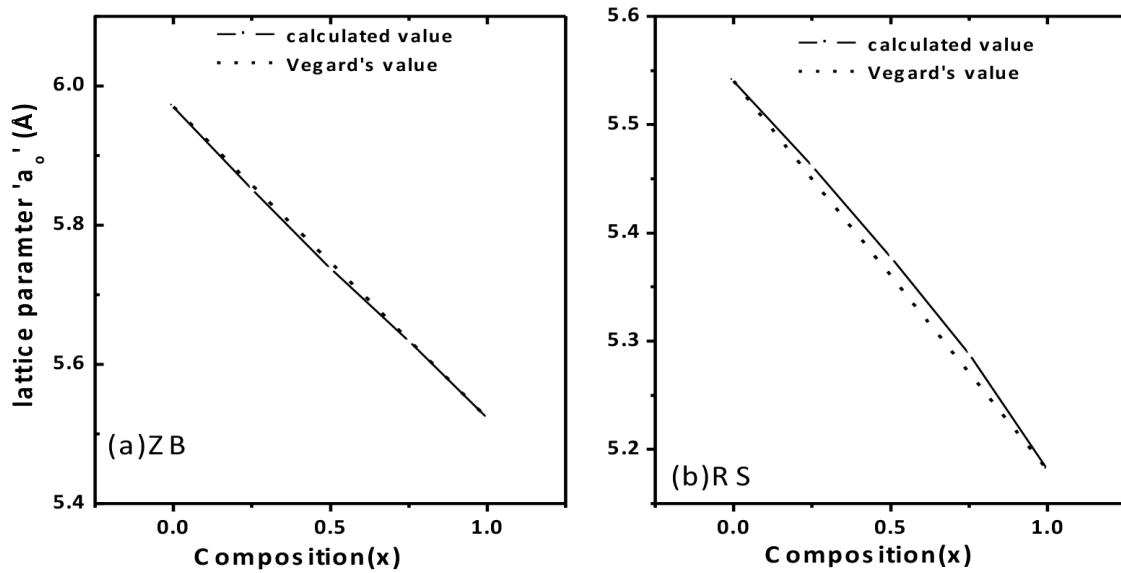


Figure 2. Composition dependence of lattice parameter a_0 as compared with Vegard's prediction: (a) ZB and (b) RS structure.

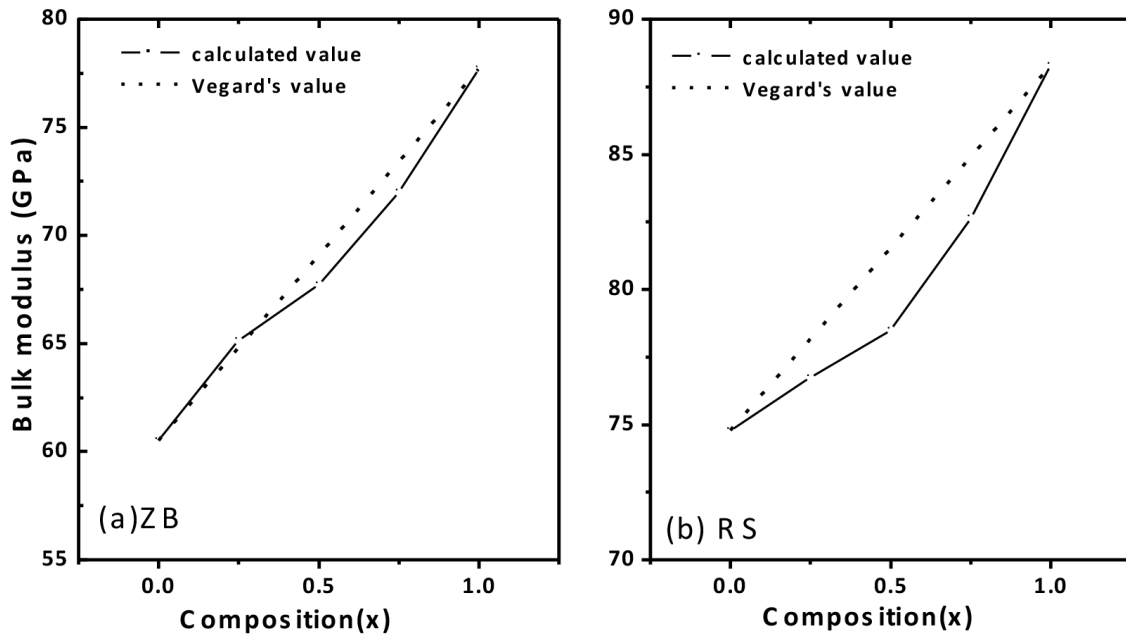


Figure 3. Composition dependence of bulk modulus as compared with Vegard's prediction: (a) ZB and (b) RS structure.

zinc-blende and the rock-salt phase, respectively. This deviation may be due to the bulk modulus mismatch between InP and GaP.

Furthermore, with an increase in concentration, the lattice constant of the alloy decreases while the bulk modulus increases. One of the reasons may be the bond strengthening effects induced by doping the Ga atom in the InP compound. In another sense, the compressibility decreases as concentration x increases in the alloys. Thus, compressibility from high to low is as follows: $\text{InP} > \text{In}_{0.75}\text{Ga}_{0.25}\text{P} > \text{In}_{0.5}\text{Ga}_{0.5}\text{P} > \text{In}_{0.25}\text{Ga}_{0.75}\text{P} > \text{GaP}$. The formation energy (E_f) of the $\text{In}_{1-x}\text{Ga}_x\text{P}$ alloys is also determined using the following relationship:

$$E_f = E_{In_{1-x}Ga_xP} - [(1-x)E_{InP} + xE_{GaP}]. \quad (3)$$

The calculated formation energy of alloys $In_{0.75}Ga_{0.25}P$, $In_{0.5}Ga_{0.5}P$, and $In_{0.25}Ga_{0.75}P$ are 0.07 eV, 0.055 eV, and 0.039 eV for the zinc-blende structure and 0.072 eV, 0.057 eV, and 0.015 eV for the rock-salt structure, respectively. Thus, the formation energy of the alloys ($x = 0.25, 0.5, 0.75$) decreases with an increase in the concentration of the Ga atom. Therefore, there is ease of formation of the alloy towards the end compound (GaP). The structural phase transitions of the alloys from ZB to RS (B3→B1) phase at different compositions are determined by calculating the Gibbs free energy, G . The phase with the lowest Gibbs energy at a given pressure and temperature determines the enthalpy of the phase. Since our calculation is done at zero temperature, we ignore the entropy contribution. Therefore, the structural phase transition is calculated from the condition of equal enthalpies, i.e. $H = E + PV$. The calculated enthalpy at different pressures for the alloys is shown in Figures 4a–4e, thus obtaining the phase transition pressure (P_t). The phase transition pressures of InP and GaP compounds are in close agreement with other experimental and theoretical results [41–50], as shown in Table 2. In cases where the experimental and theoretical data are not available at certain concentrations ($x = 0.25, 0.50, \text{ and } 0.75$), the present result may serve as a reference for further experimental work. Consequently, the introduction of the Ga atom at the site of InP increases the transition pressure. The possible reason is that the In atoms are replaced by Ga atoms in the unit cell structure of the alloy, resulting in an increase of bulk modulus, and hence the rigidity of the lattice increases. Thus, there is an increase in transition pressure.

Table 2. Transition pressure of $In_{1-x}Ga_xP$ alloys ($x = 0.0, 0.25, 0.50, 0.75, 1$).

Alloys	Phase transition (P_t) GPa		
	Pres. work	Expt. results	Theo. results
InP	9.3	9.5 ⁸ , 10.3 ⁹ , 9.8 ²²	7.3 ⁴¹ , 7.5 ⁴² , 8.5 ⁴³ , 11.0 ⁴⁴
$In_{0.75}Ga_{0.25}P$	11.4	-	-
$In_{0.5}Ga_{0.5}P$	15.7	-	-
$In_{0.25}Ga_{0.75}P$	21.2	-	
GaP	21.9	22.0 ⁴⁵ , 24.0 ⁴⁶ , 21.5 ⁴⁷	21.7 ⁴⁸ , 18.8 ⁴⁹ , 16.8 ⁵⁰

3.2. Electronic structure

Figures 5a–5e show the energy band diagram of $In_{1-x}Ga_xP$ alloys ($x = 0.0, 0.25, 0.50, 0.75, 1$) in the zinc-blende crystal structure.

In Figure 5a, the energy band diagram of InP (at $x = 0.0$), the minimum of the conduction band, and the maximum of the valence band are observed at the same Γ point. Thus, it is a direct band gap. Figures 5b, 5c, and 5d show the similar nature of the direct band gap of 1.46 eV, 1.44 eV, and 1.37 eV for $In_{0.75}Ga_{0.25}P$, $In_{0.5}Ga_{0.5}P$, and $In_{0.25}Ga_{0.75}P$ alloys, respectively. There is a trend of decrease in the band gap of the alloys as the concentration of doping increases from 25% to 75%. One of the possible results for the decrease in the band gap may be the structural relaxation of the alloy and charge exchange that are respectively proportional to the difference in the atomic orbital sizes. At 100% doping concentration ($x = 1$), the alloy becomes a binary compound that is GaP. Figure 5e shows the energy band diagram of GaP, in which the conduction band minimum lies between Γ and X symmetry points, whereas the valence band maximum lies at the Γ point. It

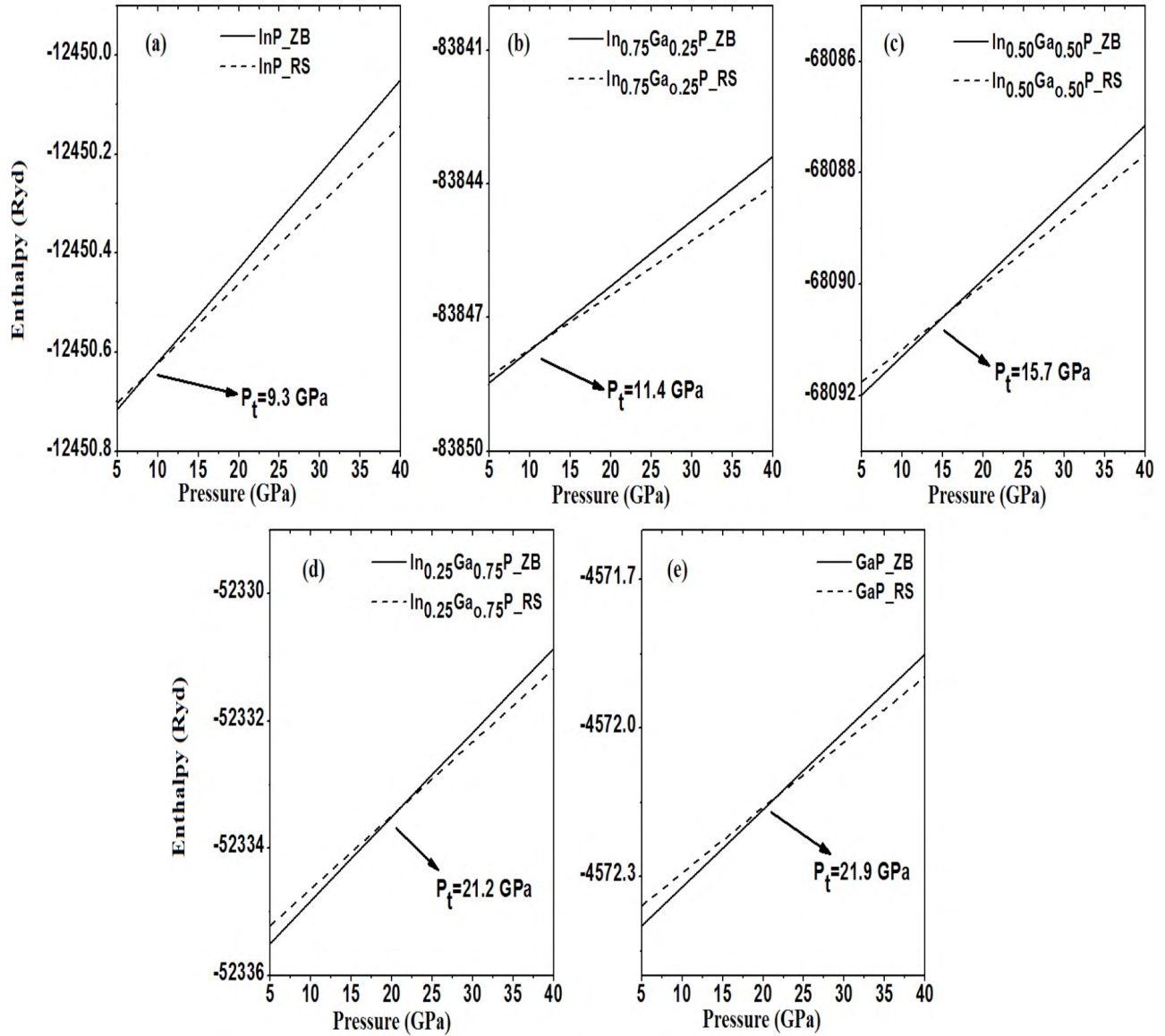


Figure 4. (a, b, c, d, e) Enthalpy versus pressure of $\text{In}_{1-x}\text{Ga}_x\text{P}$ alloys ($x = 0.0, 0.25, 0.5, 0.75, 1$).

shows that GaP is an indirect band gap compound. This is in agreement with the expected results as GaP in the zinc-blende structure is an indirect band gap semiconductor. This transition from the direct to indirect band gap may be due to strong hybridization of the Ga atom and P atom resulting in the splitting of the conduction band at the Γ point, producing another conduction band minimum between the Γ -X points attributed to an indirect band gap [51]. We also calculate the total density of states and partial density of states of the alloys as shown in Figures 6a–6e. DOS calculation shows that the s -orbital of the In atom and p -orbital of the P atom mainly contributes to the conduction band. As the doping concentration increases, the contribution of the s -orbital of the Ga atom in the conduction band increases while the p -orbital of the P atom, p -orbital of the Ga atom, and p -orbital of the In atom contribute to the valence band. In the process, all the In atoms are replaced by Ga atoms, and thus the contribution of the s -orbital of the Ga atom and p -orbital of the P atom along with

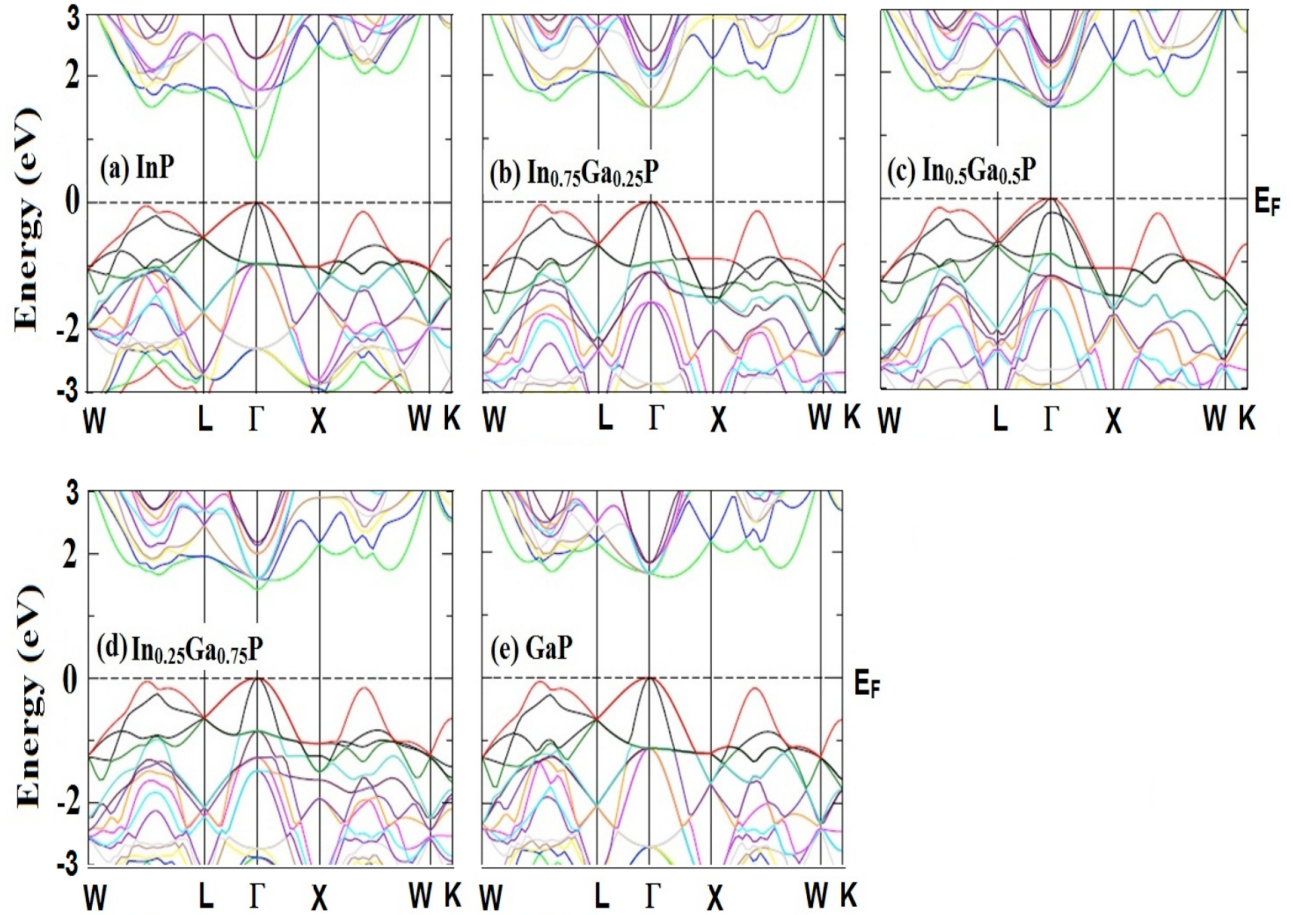


Figure 5. (a, b, c, d, e) Energy band diagram of $\text{In}_{1-x}\text{Ga}_x\text{P}$ alloys ($x = 0.0, 0.25, 0.5, 0.75, 1$) in ZB phase.

the p -orbital of the Ga atom increases in the conduction band. Figures 7a–7e are energy band diagrams of the alloys in the rock-salt crystal structure. In the band diagrams, there is a crossover of conduction and valence bands at the Fermi level. This shows that the alloys in the rock-salt structure exhibit a metallic nature.

4. Conclusions

The optimized structural parameters such as lattice constant and bulk modulus of the $\text{In}_{1-x}\text{Ga}_x\text{P}$ alloys ($x = 0.0, 0.25, 0.50, 1$) in the zinc-blende and rock-salt structures have a linear dependence obeying Vegard's law. The bulk modulus of the alloy increases with an increase in doping concentration. The InP compound has higher strength when doped with Ga atoms in replacement of In atoms in the unit cell structure. Thus, higher doping concentration in the alloy makes it less compressible. The structural phase transition pressure of the alloys under induced pressure from zinc-blende to rock-salt structure is found to increase with an increase in doping concentration. The energy band diagram of the alloys in the zinc-blende structure shows a direct band gap compound. However, at 100% doping concentration, it becomes an indirect band gap compound. This shows that the GaP in the zinc-blende structure is an indirect band gap compound. The rock-salt structure of the alloys exhibits a metallic nature.

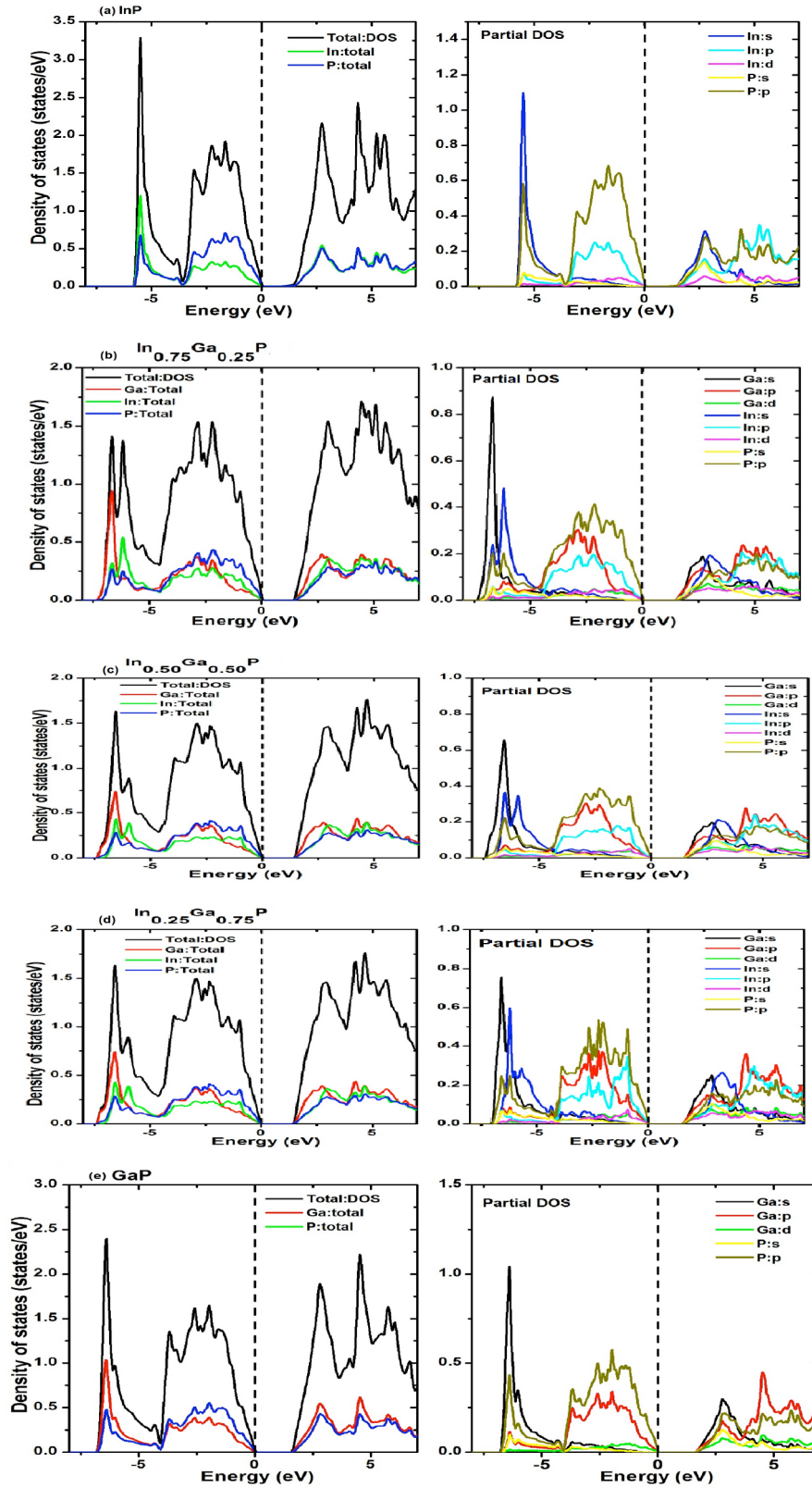


Figure 6. (a, b, c, d, e) Total and partial DOS of (a) InP-ZB phase, (b) $\text{In}_{0.75}\text{Ga}_{0.25}\text{P}$ -ZB phase, (c) $\text{In}_{0.50}\text{Ga}_{0.50}\text{P}$ -ZB phase, (d) $\text{In}_{0.25}\text{Ga}_{0.75}\text{P}$ -ZB phase, (e) GaP-ZB phase.

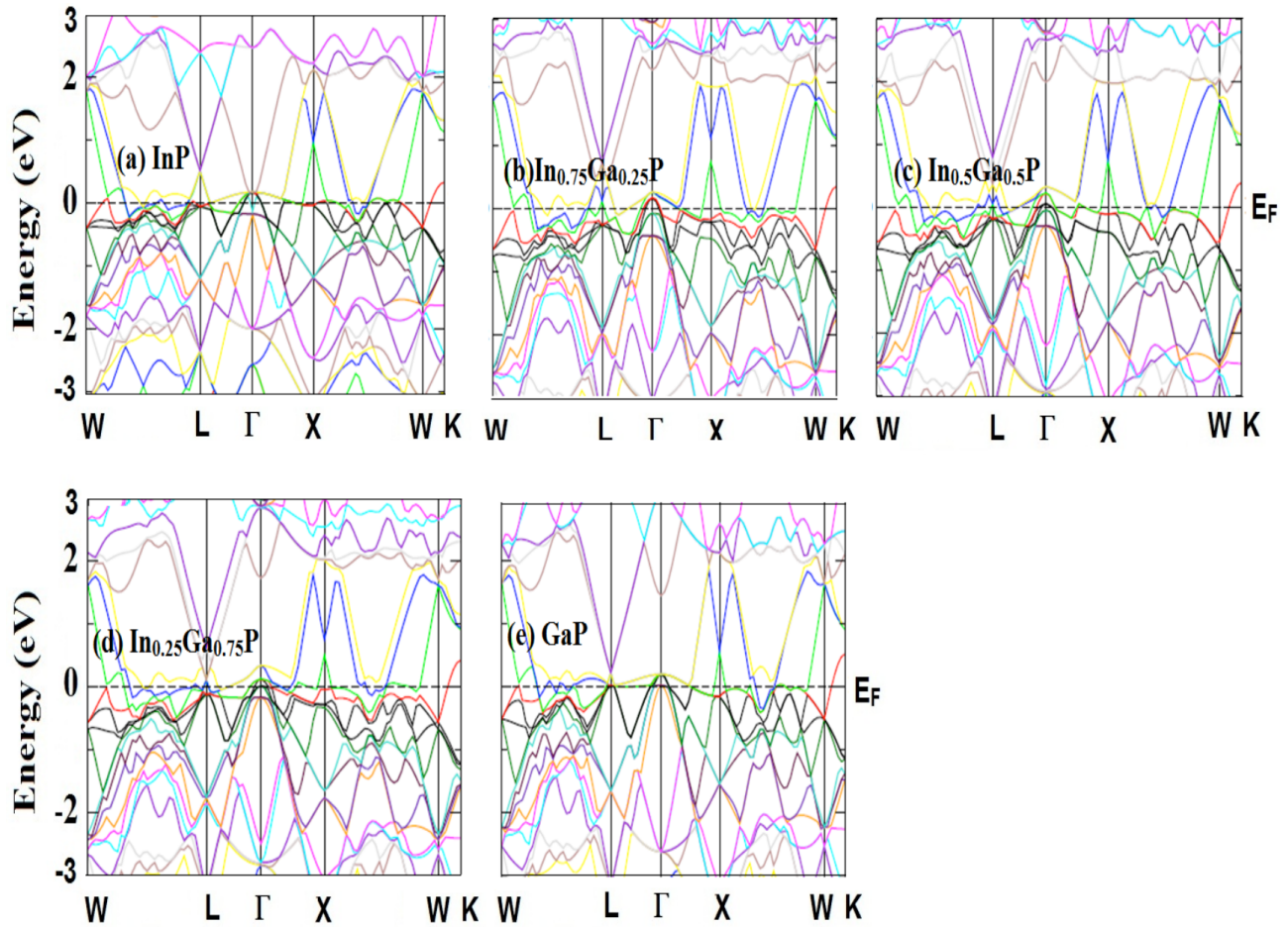


Figure 7. (a, b, c, d, e) Energy band gap of $\text{In}_{1-x}\text{Ga}_x\text{P}$ alloys ($x = 0.0, 0.25, 0.5, 0.75, 1$) in RS phase.

Acknowledgment

The authors are grateful to Dr Tilak Das and Professor Tanusri Saha-Dasgupta, SN Bose National Centre for Basic Sciences, Kolkata, India, for providing the computational facility for this work.

References

- [1] Diaz, J. G.; Bryant, G. W.; Jaskolski, W.; Zielinski, M. *Phys. Rev.* **2007**, *B75*, 245433.
- [2] Sukit, L.; Reunchan, P.; Janotti, A.; Chris, G. V. W. *Phys. Rev.* **2008**, *B77*, 195209.
 1. Raad, B. R.; Sharma, D.; Nigam, K.; Kondekar, P. *Journal of Computational Electronics* **2017**, *16*, 24-29.
- [3] Vohra, Y. K.; Weir, S. T.; Ruoff, A. L. *Phys. Rev.* **1985**, *B31*, 7344-7348.
- [4] Besson, J. M.; Itie, J. P.; Polian, A.; Weil, G.; Mansot, J. L.; Gonzales, J. *Phys. Rev.* **1991**, *B44*, 4214-4234.
- [5] Sjakste, J.; Vast, N.; Tyuterev, V. *Phys. Rev. Lett.* **2007**, *99*, 236405.
- [6] Schilling, S.; Shelton, R. N. *Physics of Solids under High Pressure*; North-Holland: New York, NY, USA, 1981
- [7] Menoni, C. S.; Spain, I. L. *Phys. Rev.* **1987**, *B35*, 7520-7525.

- [8] Arbouche, O.; Belgoumene, B.; Soudinia, B.; Azzaz, Y.; Bendaoud, H.; Amara, K. *Comput. Mater. Sci.* **2010**, *47*, 685-692.
- [9] Richards, R. D.; Harun, F.; Cheong, J. S. In *Conference Records of the IEEE Photovoltaic Specialists Conference*; IEEE: New York, NY, USA, 2016, pp. 1135-1137.
- [10] Liu, L.; Wei, J. J.; An, X. Y.; Wang, X. M.; Liu, H. N.; Wu, W. D. *Chin. Phys. B* **2011**, *20*, 106201.
- [11] Sohrabi, L.; Boochani, A.; Sebt, S. A.; Elahi, S. M. *European Physical Journal Plus*, **2018**, *133*, 117.
- [12] Mujica, A.; Needs, R. J. *Phys. Rev. B* **1997**, *55*, 9659-9670.
- [13] Wimmer, E.; Krakauer, H.; Weinert, M.; Freeman, A. J. *Phys. Rev.* **1981**, *B24*, 864-875.
- [14] Hohenberg, P.; Kohn, W. *Phys. Rev.* **1964**, *136*, 864-871.
- [15] Kohn, W.; Sham, L. J. *Phys. Rev.* **1965**, *140*, 1133-1138.
- [16] Cottenier, S. *Density Functional Theory and the Family of (L)APW-Methods: A Step-by-Step Introduction*; Instituut voor Kern-en Stralingsfysica: Leuven, Belgium, 2002.
- [17] Perdew, J. P.; Burke, S.; Ernzerhof, M. *Phys. Rev. Lett.* **1996**, *77*, 3865-3868.
- [18] Blaha, P.; Schwarz, K.; Madsen, G. K. H.; Kvasnicka, D.; Luitz, J. *WIEN2k: An Augmented Plane Wave + Local Orbitals Program for Calculating Crystal Properties*; Technical University of Vienna: Vienna, Austria, 2001.
- [19] Birch, F. *J. Appl. Phys.* **1938**, *9*, 279-288.
- [20] Madelung, O. *Semiconductors Physics of Group IV Elements and III-V Compounds, Landolt-Bornstein, New Series, Group III, Vol. 17, Part A*; Springer-Verlag: Berlin, Germany, 1982.
- [21] Kalvoda, S.; Paulus, B.; Flude, P.; Stoll, H. *Phys. Rev. B* **1997**, *55*, 4027-4030.
- [22] Seidl, A.; Gorling, A.; Vogl, P.; Majewski, J. A.; Levy, M. *Phys. Rev. B* **1996**, *53*, 3764-3774.
- [23] Nichols, D. N.; Rimia, D. S.; Sladek, R. J. *Solid State Commun.* **1980**, *36*, 667-669.
- [24] Yousaf, M.; Saeed, M. A.; Ahmed, R.; Alsardia, M. M.; Isa, A. R. M.; Shaari, A. *Commun. Theor. Phys.* **2012**, *58*, 777-784.
- [25] Ahmed, R.; Fazal-e-Aleem; Hashemifar, S. J.; Ak-Barzadeh, H. *Physica* **2008**, *B403*, 1876-1881.
- [26] McMahon, M. I.; Nelmes, R. J.; Wright, N. G.; Allan, D. R. In *Proceedings of the Joint Conference on the AIRATP/APS On High-Pressure Science and Technology*; 1993, p. 629.
- [27] Kuriyama, K.; Miyamoto, Y.; Okada, M. *J. Appl. Phys.* **1999**, *85*, 3499-3502.
- [28] Al-Douri, Y.; Ali-Hussain, R. *Appl. Phys. A* **2011**, *104*, 1159-1167.
- [29] Moss, D. J.; Ghahramani, E.; Sipe, J. E.; Van Driel, H. M. *Phys. Rev. B* **1986**, *34*, 8758-8770.
- [30] Lichanot, A.; Causa, M. *J. Phys. Condens. Matter* **1997**, *9*, 3139-3149.
- [31] Ahmed, R. R.; Aleem, F.; Hashemifar, S. J.; Akbarzadeh, H. *Physica B Condens. Matter* **2008**, *403*, 1876-1881.
- [32] Vegard, L. Z. *Journal of Physics* **1921**, *5*, 393-395.
- [33] Denton, R. A.; Ashcroft, N. W. *Phys. Rev. A* **1991**, *43*, 3161-3164.
- [34] Jobst, B.; Hommel, D.; Lunz, U.; Gerhar, T.; Landwehr, G. *Applied Physics Letters* **1996**, *69*, 97-100.
- [35] Hassan, F. E. H.; Akbardadeh, H. *Materials Science and Engineering B* **2005**, *121*, 170-177.
- [36] Al-Douri, Y. *Solid State Commun.* **2004**, *132*, 465-470.
- [37] Al-Douri, Y. *Journal of Applied Physics* **2003**, *93*, 9730-9736.
- [38] Al-Douri, Y. *Materials Chemistry and Physics* **2003**, *82*, 49-54.
- [39] Al-Douri, Y.; Mecabih, S.; Benosman, N.; Aourag, H. *Physica B* **2003**, *325*, 362-371.

- [40] Lukacevic, I.; Kirin, D.; Jha, P. K.; Gupta, S. K. *Phys. Status Solidi* **2010**, *B247*, 273-277.
- [41] Chenghua, H.; Wang, F.; Zheng, Z. *J. Mater. Res.* **2012**, *27*, 1105-1111.
- [42] Singh, R. K.; Singh, S. *Phys. Rev.* **1989**, *B39*, 671-676.
- [43] Zhang, S. B.; Cohen, M. L. *Phys. Rev.* **1987**, *B35*, 7604-7610.
- [44] Millers, A. J.; Saunders, G. A.; Yogurtcu, Y. K. *J. Phys. Chem. Solids* **1981**, *42*, 49-56.
- [45] Pinceaux, J. P.; Besson, J. M.; Rimsky, A.; Weil, G.; Editors. *High Pressure in Research and Industry. Proceedings of the 8th AIRAPT Conference*; Institute of Physical Chemistry: Uppsala, Sweden, 1981.
- [46] Baublitz, M.; Ruoff, A. L. *J. Appl. Phys.* **1982**, *53*, 6179-6185.
- [47] Froyen, S.; Cohen, M. L. *Solid State Commun.* **1982**, *43*, 447-450.
- [48] García, A.; Cohen, M. L. *Phys. Rev. B* **1993**, *47*, 6751-6754.
- [49] Ozoli s, V.; Zunger, A. *Phys. Rev. Lett.* **1999**, *82*, 767-770.
- [50] Bouarissa, N.; Baazis, H.; Charifi, Z. *Phys. Status Solidi B* **2002**, *231*, 403-410.